Available online at www.sciencedirect.com
ScienceDirect
Journal of Molecular Catalysis A: Chemical 267 (2007) 209–217
JOURNAL OF MOLECULAR CATALYSIS A: CHEMICAL
www.elsevier.com/locate/molcata

Hydroisomerization of ethylbenzene over bimetallic bifunctional zeolite catalysts

A. Geetha Bhavani [a], A. Pandurangan [a,b,*]

[a] *Department of Chemistry, Anna University, Chennai 600042, India*
[b] *CAER, University of Kentucky, Lexington, KY 40511-8410, United States*

Received 24 April 2006; received in revised form 18 November 2006; accepted 21 November 2006
Available online 28 November 2006

Abstract

Zeolite-β and mordenite were impregnated with 0.1 wt.% Pt and varying (0, 0.1, 0.3, 0.5 wt.%) amount of Ni. The line broadening XRD analysis indicates that the increasing Ni addition decreases the crystallinity of zeolites. The TEM analysis indicates that the average metal particle size increases with increasing Ni addition. The states of Ni and Pt were analyzed by ESCA. The acidity measurements by both TPD of ammonia and pyridine adsorbed FT-IR spectroscopy show the occupation of some of the acid sites by the added Ni species. Ni addition up to 0.3 wt.% over 0.1 wt.% Pt/H-β and 0.1 wt.% over 0.1 wt.% Pt/H-MOR enhances the ethylbenzene conversion, isomerization selectivity and sustainability of the catalysts. Further Ni addition above the threshold value leads to a drastic drop in activity and isomerization selectivity. Zeolite-β-based Ni–Pt catalysts always show higher activity and selectivity than mordenite-based catalysts.

Keywords: Hydroisomerization; Ethylbenzene; Nickel; Platinum; Zeolite-β; Mordenite

1. Introduction

Isomerization of C_8 aromatic is an important industrial process by which the discrepancy between the requirements of *para* xylene and its production from original sources can be solved. C_8 aromatic hydrocarbon results from naphtha reforming and steam cracking contains not only ethylbenzene but also xylene, the separation of which is very expensive. Isomerization of ethylbenzene into xylene, however, is a more complicated reaction that requires a bifunctional catalyst [1]. The acid and metal site density and strength distribution are both important and their proper balance is critical in determining the acidity of these catalysts [2–4]. It was found that the introduction of a second metal influences the property of the first dispersed metal due to the formation of metallic clusters [5]. Moreau et al. [6] carried out EB transformation on bifunctional catalyst Pt/Al_2O_3 associated with NaHMOR samples at 410 °C and showed that the exchange of the mordenite causes a significant increase in the selectivity to isomers of the bifunctional catalysts due to significant decrease in secondary reactions. Robschlger and Christoffel [7] studied weakly acidic Pt/Al_2O_3 and Pt zeolite with higher acidity using the pulse micro-catalytic technique and reported that on Pt-zeolite 2.23, 5.11 and 1.77% of *o*-, *m*-, *p*-xylenes were formed at 400 °C. Over bimetallic bifunctional catalysts, Jordao et al. [8] accounted for the higher activity of Ni–Pt catalysts by (i) the presence of Pt enhancing the reduction of Ni cations forming more metal particles, (ii) the Ni particles serving as support for the Pt atoms and (iii) the generation of higher superficial energy due to difficulty in accommodation of Pt atoms in Ni metal particles. The enhanced activity was accounted for in terms of better metal–acid site balance between catalytically active bimetallic (Ni–Pt) nanoparticles formed and the acid sites of the support. Catalysts with higher Ni content show poor activity due to pore blockage by larger bimetallic particles formed and incomplete reduction of nickel species.

Hence this study is undertaken with a view to maximize selectivity of xylene isomers using Ni addition to Pt loaded zeolites (β and mordenite) to rationalize the variations in the product distributions in terms of effect of Ni loading over zeolite supports, acidity of the supports, reaction temperature and stability of catalysts.

* Corresponding author at: CAER, University of Kentucky, Lexington, KY 40511-8410, United States. Tel.: +1 859 257 0250; fax: +1 859 257 0302.
E-mail address: pandurangan_a@yahoo.com (A. Pandurangan).

1381-1169/$ – see front matter © 2006 Elsevier B.V. All rights reserved.
doi:10.1016/j.molcata.2006.11.044

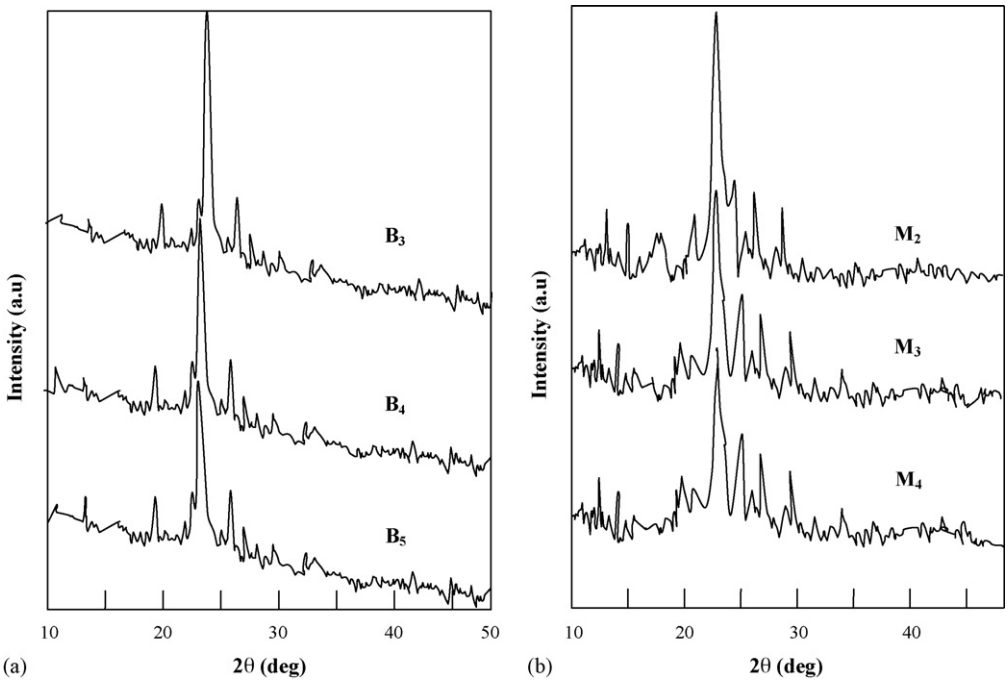

Fig. 1. (a) Line broadening XRD pattern of catalysts B_3, B_4 and B_5. (b) Line broadening XRD pattern of catalysts M_2, M_3 and M_4.

2. Experimental

2.1. Catalyst preparation

The H-form of zeolite-β ($SiO_2/Al_2O_3 = 10$) and mordenite ($SiO_2/Al_2O_3 = 12.5$) was supplied by United Catalyst India Ltd., India. Aqueous solutions of chloroplatinic acid and nickel nitrate were used as sources of Pt and Ni, respectively. The H-forms of zeolite-β and mordenite were loaded with 0.1 wt.% Pt the by incipient wetness impregnation (IWI) and the resulting materials are designated as catalysts B_1 and M_1, respectively. Parts of catalyst B_1 were separately impregnated with 0.1, 0.3 and 0.5 wt.% Ni and the resulting samples are designated as B_2, B_3 and B_4, respectively. Similarly 0.1, 0.3 and 0.5 wt.% Ni was impregnated over M_1 and the product materials are designated as M_2, M_3 and M_4, respectively. For comparison purposes 0.3 wt.% Ni, 0.1 wt.% Pt/H-β, and 0.1 wt.% Ni, 0.1 wt.% Pt/H-MOR were prepared by the ion-exchange method (IE) and the resulting materials are designated as catalysts B_5 and M_5, respectively. Catalysts 0.4 wt.% Ni/H-β and 0.2 wt.% Ni/H-MOR were also prepared by IWI method and are designated as catalysts B_6 and M_6, respectively. The metal loaded catalysts were dried at 120 °C for 12 h. Each of the earlier mentioned catalysts (1 g each) were packed in a quartz reactor and activated at 550 °C for 3 h under N_2 atmosphere. Then the temperature was lowered to 475 °C under hydrogen flow (30 ml/(min g)) for 6 h in order to reduce the metal ions.

2.2. Characterization

The catalysts were previously characterized by line broadening XRD as well as TEM, ESCA, TGA-TPD, pyridine adsorbed FT-IR and catalytic studies were mentioned in our previous report [9].

3. Results and discussion

3.1. Characterization

3.1.1. Line broadening XRD

The XRD pattern of zeolite-β exhibits the most intense diffraction peaks at $2\theta = 20–32^\circ$ and thus confirms the BEA structure as well as its good crystalline nature. The XRD pattern of mordenite obtained show sharp peaks between the 2θ values 6–30° indicating the presence of MOR structure. Line broadening XRD patterns obtained for catalysts B_3, B_4 and B_5 (B series) and M_2, M_3 and M_4 (M series) are shown in Fig. 1(a) and (b), respectively. The intensity of the XRD peaks is found to decrease with increasing Ni addition in both the systems. By using Cu Kα X-ray, the intense peaks of Pt, Ni (cubic) and NiO (hexagonal) are expected at the 2θ values of 39.8°, 44.5° and 43.3°, respectively. But in the present case, all the above peaks are missing which may be due to the low concentration of Pt as well as Ni species. The decrease in XRD peak intensities attributed to the supports and may be due to increasing pore blockage of support materials by the added Ni species.

3.1.2. TEM analysis

The TEM pictures of catalysts B_3, B_4, M_2 and M_3 are in shown Fig. 2(a) and (b), respectively. The black dots seen on the support matrix are bimetallic (Ni–Pt) particles on the surface of the supports. The average size of the particles on each support was determined and presented in Table 1. It was observed from our previous report that in case of Ni–Pt/H-Y [9], the average

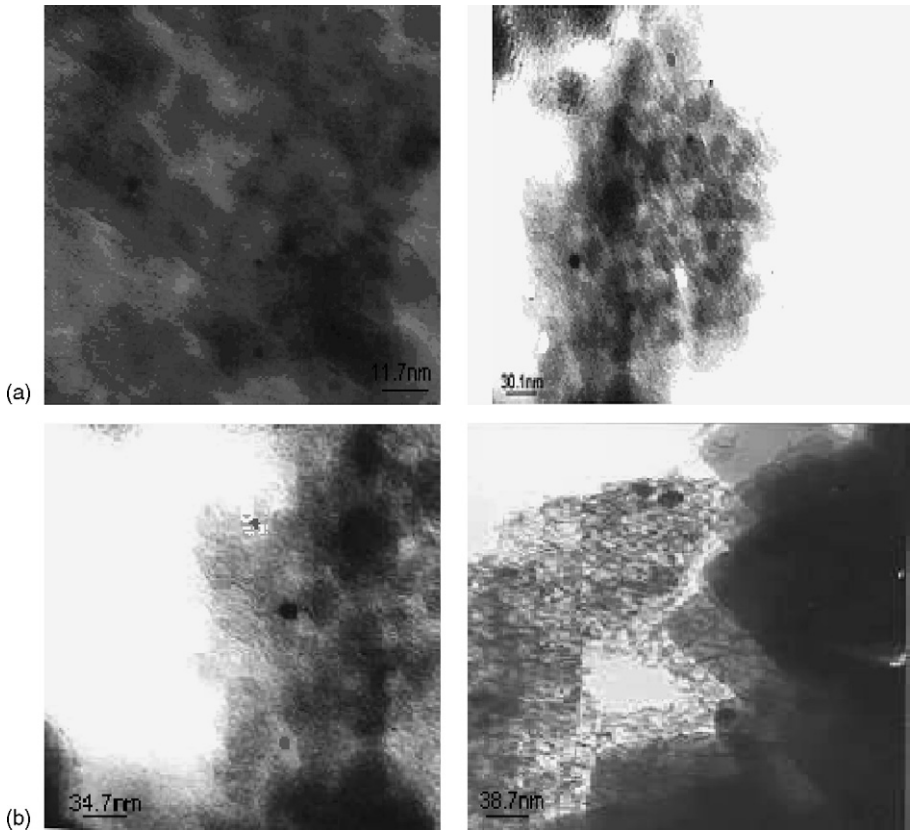

Fig. 2. (a) TEM picture of catalysts B_3 and B_4. (b) TEM picture of catalysts M_2 and M_3.

particle size is found to increase with increasing Ni addition. The average particle size of catalysts B_3 and M_2 are found to be 4.55 and 3.71 nm, respectively, and that of catalysts B_4 and M_3 are 10.78 and 5.42 nm, respectively. Such particles may be larger in size compared to the pores of zeolite supports. Canizares et al. [10] and Ostard et al. [11] used TEM to study the effect of Ni loading technique on the particle size of the Ni/MOR catalysts and observed that large particles are always formed outside the zeolite crystals, regardless of metal loading technique (ion-exchange and impregnation). From the current observation Ni–Pt particle of definite size grows further on the addition of Ni is possible only because of the migration of Ni particles during the reduction.

3.1.3. ESCA

The ESCA spectra of Pt and Ni species in reduced catalysts B_3, B_4, M_3 and M_4 are shown in Fig. 3. In the case of Pt, two major peaks are observed irrespective of the support and the

Table 1
Physiochemical characteristics of B and M series catalysts

S. no.	Catalyst	Pt content (wt.%)	Ni content (wt.%)	BET surface area (m^2/g)	NH_3-TPD (mmol/g)		Total acidity (mmol/g)	Particle size (nm)
					LT-peak	HT-peak		
1	B_1	0.1	–	565	0.775	0.189	0.964	–
2	B_2	0.1	0.1	527	0.763	0.172	0.935	–
3	B_3	0.1	0.3	477	0.710	0.140	0.850	4.55
4	B_4	0.1	0.5	476	0.575	0.130	0.705	10.78
5	B_5[a]	0.1	0.1	483	0.723	0.138	0.861	–
6	B_6	–	0.5	492	0.718	0.155	0.873	–
7	M_1	0.1	–	463	0.728	0.416	1.144	–
8	M_2	0.1	0.1	405	0.644	0.212	0.856	3.71
9	M_3	0.1	0.3	360	0.634	0.177	0.811	5.42
10	M_4	0.1	0.5	326	0.625	0.172	0.797	–
11	M_5[a]	0.1	0.1	412	0.662	0.195	0.857	–
12	M_6	–	0.2	426	0.653	0.224	0.877	–

LT: low temperature peak, HT: high temperature peak.
[a] Prepared by ion-exchange method.

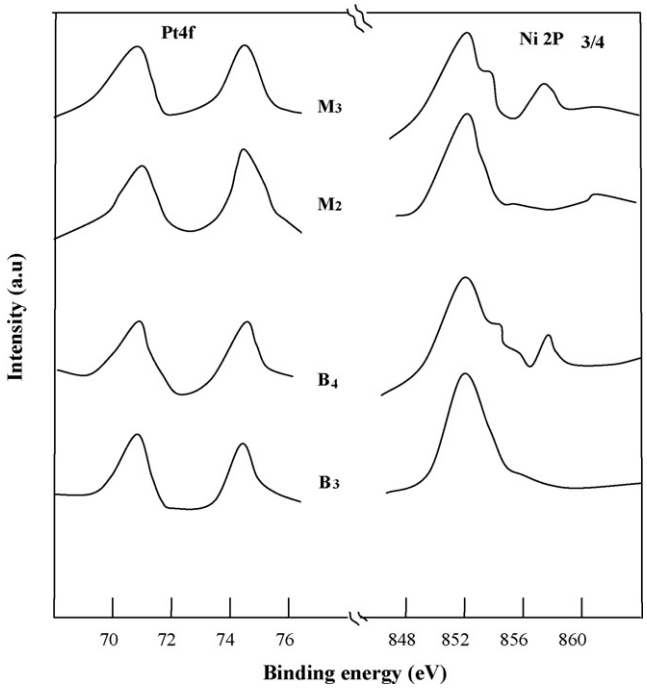

Fig. 3. ESCA spectra of catalysts B_3, B_4, M_2 and M_3.

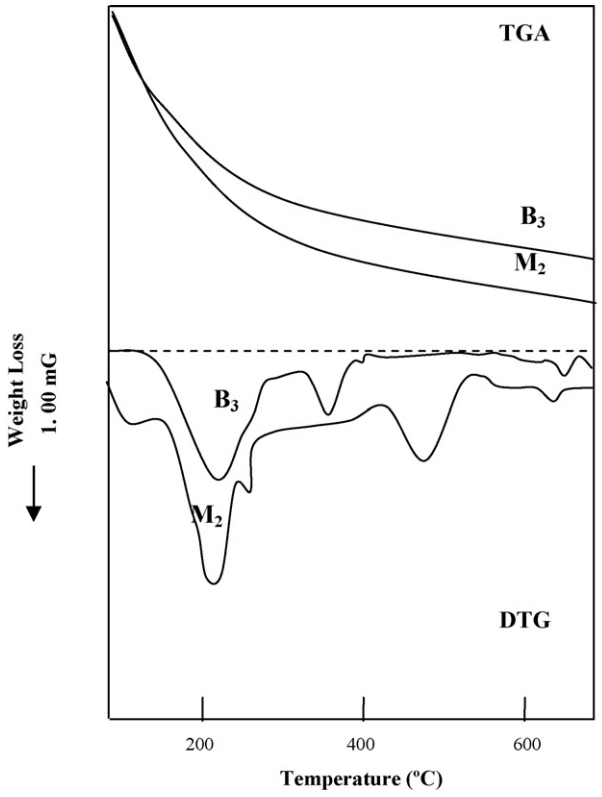

Fig. 4. Typical TGA-TPD curves of catalysts B_3 and M_2.

amount of nickel. The peaks with binding energy values of 71.0 and 74.5 eV are corresponding to the core level Pt $4f_{7/2}$ and Pt $4f_{5/2}$ transitions, respectively, indicating the presence of platinum in metallic state. However the presence of Pt in higher oxidation state cannot be discarded because of the possibility of overlap with Al 2p transition of support [12,13]. The ESCA spectra of Ni $2p_{3/2}$ peaks have two peak maxima with binding energies 852.3 and 854.0 eV indicating the presence of metallic Ni and NiO, respectively. A broad peak seen around 857.0 eV in catalysts B_4 and M_4 indicate the presence of Ni^{2+} and the formation of $NiAl_2O_4$ from which the reduction of Ni^{2+} is very difficult (Ni metal: 852.3 eV; NiO: 853.3 eV; $NiAl_2O_4$: 857.2 eV in ESCA data book) [14,15]. Thus in the present case the added Pt is postulated to favor the reduction of Ni cation in the region 0–0.3 wt.% Ni and further increasing Ni loading (0.5 wt.%) NiO is observed for B series catalysts. In M series NiO formation is observed in adding 0.3 wt.% Ni itself.

3.1.4. TGA-TPD of NH_3

The desorption of ammonia was carried out over B and M series catalysts by TGA method and the amount of ammonia desorbed from each of B and M series catalysts are presented in Table 1. The model TGA-TPD curves for the typical catalysts B_3 and M_2 are shown in Fig. 4. The temperatures of desorption and amount of ammonia desorbed are the indexes of strength and number of acid sites [16]. There are two weight losses occurring at two different temperature ranges which may be due to desorption of adsorbed ammonia on weak and strong acid sites. The first weight loss occurs in the temperature range of 200–250 °C for B and M series catalysts. The second weight loss occurs at 350–400 °C for B series catalysts and that in M series catalysts at 500–550 °C. From Table 1, it is found that the peak for low temperature desorption is always for higher than the peak higher temperature desorption. When Ni is added in increasing amount to the Pt loaded supports, the total acidity continuously falls in both the supports. When the Ni is brought into the Pt loaded zeolites by ion-exchange method, there is no significant change in acidity when compared with that of impregnated catalysts. This shows that Ni dispersion whether done by IWI or ion exchange, a definite amount of Ni occupies the acid sites and it to the growth of Pt–Ni particles. For a definite amount of Ni added, the decline in acidity is more in mordenite than zeolite-β. For example, it is observed that when 0.3 wt.% Ni is added to the supports containing 0.1 wt.% Pt, the acidity fall is more in mordenite material (0.303 mmol/g) than zeolite-β (0.114 mmol/g).

3.1.5. Pyridine adsorbed FT-IR spectroscopy

The pyridine adsorbed FT-IR spectra of B and M series catalysts are shown in Fig. 5(a) and (b), respectively. A broad peak appeared around 1545 cm^{-1} on all the catalysts indicating the presence of pyridine adsorbed on Brønsted acid sites of zeolites. The pyridine adsorption on Lewis acid sites is indicated by another peak around 1455 cm^{-1}. The increasing addition of Ni content in B and M series catalysts has no effect on the position of both Brønsted and Lewis acid site peaks but the intensity of the each peak was found to decrease indicating that the number of both Brønsted and Lewis acid sites decreases with increasing Ni loading. The decrease in the number of acid sites may be due to the occupation of acid sites by Ni species when increasing metal loading as observed in TPD-NH_3 studies. A sharp peak obtained around 1490 cm^{-1} indicates the physically adsorbed pyridine. The BET surface area (Table 1) of the both B and M series catalysts show a decreasing trend with increasing Ni addition,

Table 2
Product distribution (wt.%) in ethylbenzene hydroisomerization over B series catalysts

Product (wt.%)	250 °C						300 °C					
	B_1	B_2	B_3	B_4	B_5	B_6	B_1	B_2	B_3	B_4	B_5	B_6
Benzene	6.5	6.2	6.3	6.1	6.3	6.2	8.9	9.1	9.3	9.2	9.5	9.1
Toluene	1.5	1.5	1.7	1.3	1.6	1.7	2.2	2.3	2.4	2.2	2.2	2.1
Xylene	13.5	19.6	22.2	17.5	15.4	10.5	21.3	32.3	36.2	28.5	25.3	16.7
ET	1.6	1.7	1.5	1.2	1.4	1.7	3.4	2.3	3.2	3.0	3.2	3.5
TMB	1.4	1.3	0.8	1.4	1.3	1.5	1.7	1.4	1.5	1.3	2.6	2.7
DEB	3.7	3.9	4.1	3.4	3.8	3.9	9.1	9.0	8.7	8.0	8.6	9.1
Naphthenes	3.2	3.1	3.2	3.0	3.3	4.3	6.1	6.3	6.8	5.5	5.4	6.5
Conversion	31.4	37.3	39.8	33.9	33.1	28.8	52.7	62.7	68.1	57.7	56.8	49.7
Isomerization selectivity	42.4	52.5	55.8	51.6	46.5	36.5	39.9	51.4	53.2	49.4	45.4	33.6
	350 °C						400 °C					
	B_1	B_2	B_3	B_4	B_5	B_6	B_1	B_2	B_3	B_4	B_5	B_6
Benzene	8.1	10.2	9.0	9.3	9.7	8.2	6.5	6.7	7.8	7.7	7.3	7.0
Toluene	2.3	2.6	2.5	2.2	2.4	2.6	2.4	2.7	2.3	2.5	2.4	2.6
Xylene	21.6	31.1	35.7	27.2	25.0	16.7	21.7	30.6	34.1	27.5	24.0	21.3
ET	4.5	5.2	4.3	5.1	4.2	4.6	6.9	5.6	5.7	6.5	6.6	5.7
TMB	4.1	2.6	2.7	2.5	3.5	4.3	5.7	4.6	4.4	4.2	3.7	3.9
DEB	9.2	9.1	8.4	8.2	8.7	8.6	11.7	12.4	12.7	13.4	13.4	11.5
Naphthenes	9.4	8.0	7.6	8.9	9.3	10.7	9.2	10.5	10.9	7.8	11.3	8.1
Conversion	59.2	68.8	70.2	63.4	62.8	56.7	64.1	73.1	77.9	69.6	68.7	60.1
Isomerization selectivity	36.4	44.2	48.0	43.0	40.0	31.8	33.8	41.9	43.8	38.1	35.4	35.0

LHSV = 2.0 h^{-1}, H_2 flow rate = 20 ml/(min g), wt. of catalyst = 1 g, time-on-stream = 1 h.

which may reflect the observation made in acidity measurement studies.

3.2. Catalytic studies

3.2.1. Product distribution

Hydroisomerization of EB was carried out over the above bifunctional catalysts at LHSV = 2.0 h^{-1} in the temperature range 250–400 °C in the steps of 50 °C. The product distribution in EB hydroisomerization over B and M series catalysts are presented in Tables 2 and 3, respectively. These products result from five main transformations of EB:

(1) Isomerization of EB into *ortho*-, *meta*-, *para*-xylenes.
(2) Disproportionation and dealkylation of EB into benzene, trimethylbenzene (TMB) and diethylbenzene (DEB).

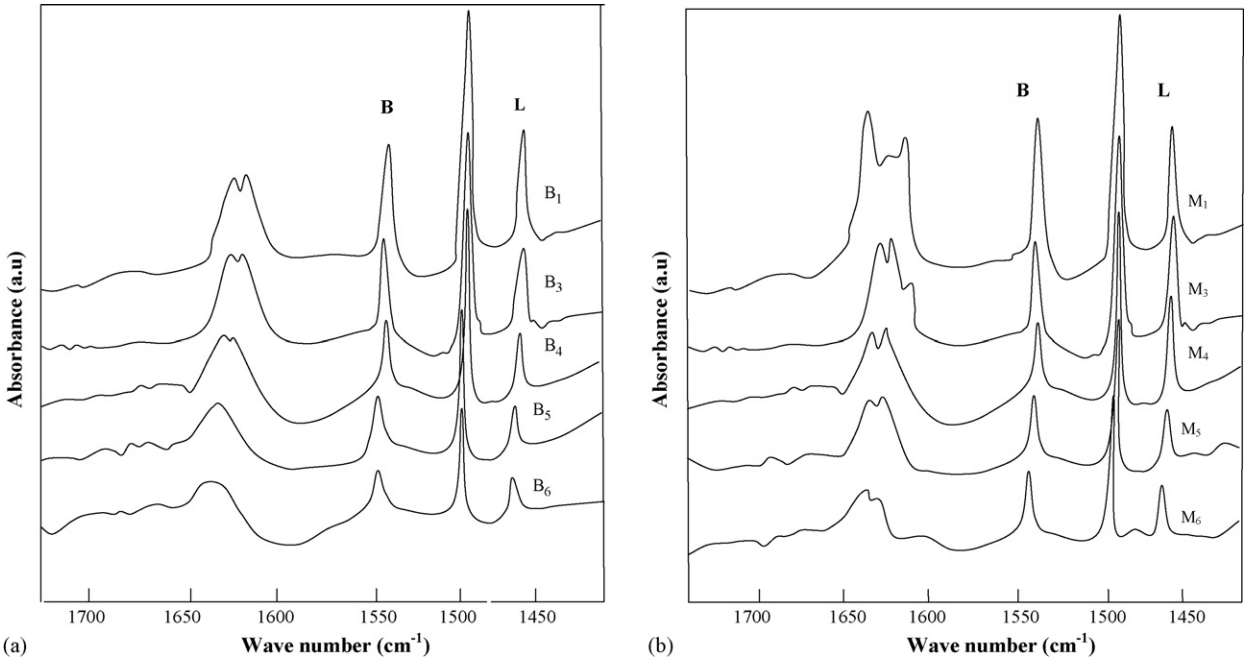

Fig. 5. (a) Pyridine adsorbed FT-IR spectra of B series catalysts. (b) Pyridine adsorbed FT-IR spectra of M series.

Table 3
Product distribution (wt.%) in ethylbenzene hydroisomerization over M series catalysts

Product (wt.%)	250 °C						300 °C					
	M_1	M_2	M_3	M_4	M_5	M_6	M_1	M_2	M_3	M_4	M_5	M_6
Benzene	2.3	5.2	3.9	2.9	3.7	1.1	10.0	7.4	9.3	9.4	8.4	8.3
Toluene	1.4	1.3	1.4	1.2	1.3	1.4	1.5	1.7	1.3	1.2	1.4	1.7
Xylene	10.8	22.9	18.3	15.4	12.8	8.4	19.4	33.5	29.3	26.5	23.6	15.2
ET	1.1	1.2	1.3	2.1	1.2	1.3	2.9	2.7	2.6	2.5	2.8	3.2
TMB	1.4	1.1	1.2	1.3	2.4	1.4	2.3	2.1	2.2	2.3	2.5	2.5
DEB	3.6	3.5	3.6	2.3	3.1	3.0	6.9	7.2	7.5	7.0	7.8	8.1
Naphthenes	4.7	4.0	4.2	4.3	4.4	4.6	9.5	9.7	9.5	9.6	10.9	9.8
Conversion	25.3	36.2	33.9	29.5	28.9	21.2	52.5	64.3	61.7	58.5	57.4	48.8
Isomerization selectivity	42.7	55	54.0	51.5	44.3	39.7	57.0	52.1	47.5	45.3	41.3	31.5
	350 °C						400 °C					
	M_1	M_2	M_3	M_4	M_5	M_6	M_1	M_2	M_3	M_4	M_5	M_6
Benzene	7.5	7.3	8.0	7.5	5.4	6.5	7.3	7.2	7.3	6.8	7.1	7.5
Toluene	1.8	1.5	1.6	1.3	1.7	2.1	1.7	1.5	1.4	1.2	1.6	1.8
Xylene	18.3	33.4	29.1	25.1	21.4	14.9	16.5	30.3	27.4	25.5	21.7	11.8
ET	4.4	5.1	5.3	3.8	4.2	4.6	4.6	5.5	4.3	4.1	4.4	4.9
TMB	2.3	2.3	2.4	3.2	3.4	2.6	3.5	2.6	3.5	3.7	3.5	4.9
DEB	8.9	8.9	8.8	9.5	10.7	9.5	12.4	12.6	12.5	11.7	12.3	11.5
Naphthenes	12.7	10.0	10.1	11.0	13.5	11.9	14.7	13.5	13.7	13.9	14.8	13.9
Conversion	55.9	68.5	65.3	61.4	60.3	52.1	60.7	73.2	70.1	66.9	65.4	56.3
Isomerization selectivity	32.7	48.6	44.6	40.9	35.5	28.6	27.2	41.4	39.1	38.1	33.2	20.9

LHSV = 2.0 h^{-1}, H_2 flow rate = 20 ml/(min g), wt. of catalyst = 1 g, time-on-stream = 1 h. ET: ethyltoluene; TMB: trimethylbenzene; DEB: diethylbenzene.

(3) Transalkylation of EB into xylene to ethyltoluene (ET) and toluene or to dimethylethylbenzene (DMEB) and benzene.
(4) Hydrogenation of C_8 aromatics (with isomerization of the products).
(5) Cracking of C_8 naphthenes (N_8) into C_3–C_6 alkanes.

3.2.2. *Effect of Ni loading over zeolite-β (B series)*

The effect of Ni loading on the conversion of EB over B series catalysts was studied in the range 0–0.5 wt.% Ni on 0.1 wt.% Pt/HY at different temperatures in the range 250–400 °C with optimized flow rate. The increase in temperature shows an increasing trend for the conversion for all the catalysts was observed. The conversion and isomerization selectivity of B series catalysts at 250 and 400 °C were shown in Fig. 6(a) and (b), respectively. At 400 °C the maximum conversion was observed and out of B series catalysts, B_3 catalyst shows maximum conversion and xylene selectivity. When the reaction temperature increases, more amounts of undesired dealkylated (naphthenes, toluene, benzene) products were observed. The increasing ethylbenzene conversion as well as isomerization selectivity with increasing Ni addition may be due to the formation and growth of catalytically active metallic particles, which may be facilitated by the presence of the added Ni. Bimetallic particles with above-mentioned average particle size are supposed to offer better synergism with acid sites of supports and favor the bimolecular mechanism proposed by Csicery [17,18].

The ion-exchanged catalyst B_5 shows less xylene selectivity with more cracked products than impregnated catalysts at all the temperatures. Satyanarayana [19] studied the transformation of C_8 aromatics on platinum, palladium and nickel supported on ZSM-5. Deactivation was rapid over nickel and palladium loaded zeolite catalysts and C_8 loss was lower on

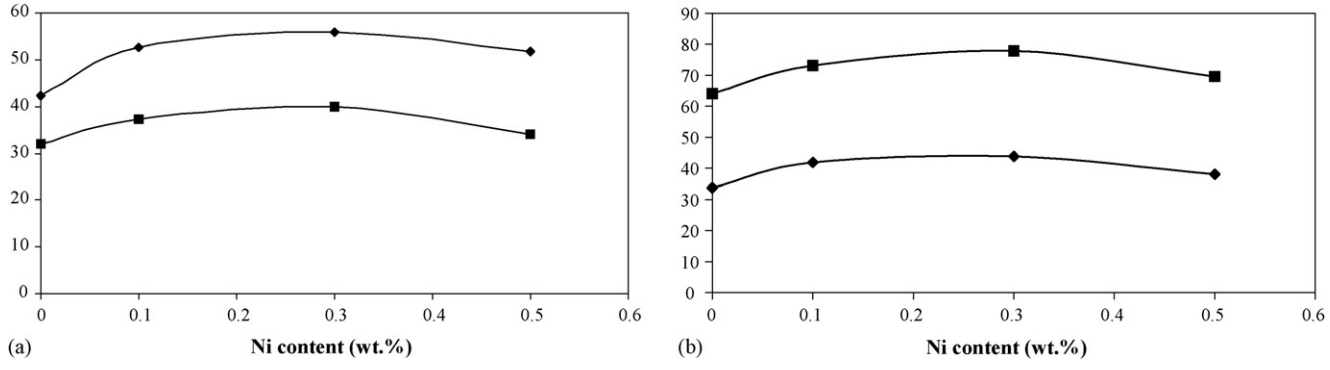

Fig. 6. (a) Effect of Ni addition on ethylbenzene conversion over B series catalysts at 250 °C (a) and 400 °C (b) temperature: (♦) isomerization selectivity and (■) conversion.

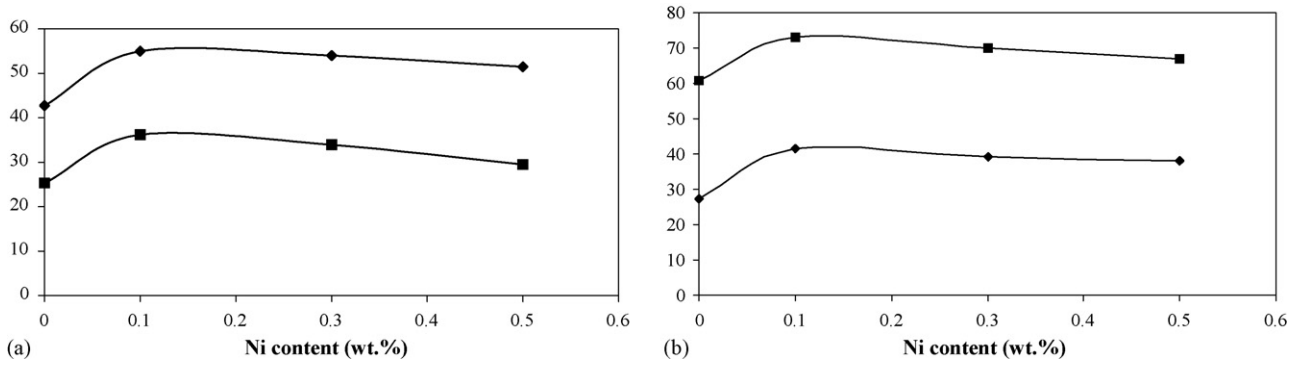

Fig. 7. (a) Effect of Ni addition on ethylbenzene conversion over M series catalysts at 250 °C (a) and 400 °C (b) temperature: (♦) isomerization selectivity and (■) conversion.

platinum zeolite catalysts. On the other hand nickel impregnated zeolite shows much higher conversion than nickel ion-exchanged zeolite due to the presence of Ni^0 in the former.

3.2.3. *Effect of Ni loading over mordenite (M series)*

For the M series of catalysts the M_2 catalyst shows the maximum conversion and xylene selectivity. The effect of Ni addition over M series catalysts on conversion and isomerization selectivity is shown in Fig. 7(a) and (b), respectively. Compared to monometallic catalysts bimetallic catalysts show the maximum conversion and selectivity towards xylenes at all the temperatures. The increasing the Ni addition and temperature over all the catalyst the undesired dealkylation and (naphthenes, toluene, benzene) products were observed.

Among two series of catalysts, zeolite-β shows the highest selectivity to desired isomerization products, i.e., xylenes. The TEM studies show that the average particle size of bimetallic particles increases with increasing Ni loading. Catalysts B_3 and M_2 have an average particle size 4.55 and 3.77 nm by TEM analysis. Also, the ESCA spectra of catalysts B_3 and M_2 show the complete reduction of Pt and Ni to the metallic state. The added Ni species may increase the total number of active metallic sites, i.e. the metallic sites/acid sites ratio may increase towards the optimum value for isomerization reactions. The decreasing conversion trend with increasing disproportionation and cracking selectivity was observed over catalysts with higher Ni content which may due to the formation of larger bimetallic particles and the presence of unreduced Ni as NiO and $NiAl_2O_4$ as evidenced by ESCA. Catalysts B_4 and M_3 have the average particle size of 10.78 and 5.42 nm by TEM analysis, such large bimetallic particles may block the pore of zeolite and restrict transport of bulk reaction intermediates [9]. Also, the presence of unreduced Ni species, which are inactive in hydrogenation–dehydrogenation steps, may disturb the synergism between metal–acid sites leading to lower activity. The decrease in crystallinity of the supports indicated by line broadening XRD is also responsible for the lower activity.

It was observed that a reduced amount of accessible Brønsted acid sites in the zeolite favored the isomerization of EB with respect to secondary reactions like cracking of naphthenes and dealkylation. Similar results were observed in case of monometallic (Pt/Ni) and ion-exchanged catalysts in all the systems. Fernandes [20] studied the influence of zeolite structure on the catalytic performance of bifunctional Pt/Al_2O_3-zeolite (MOR, β, Y, ZSM-5 and MCM-22) composites (0.45 wt.% Pt) for hydroconversion of EB at 420 °C. It was observed that large pore (β > MOR > Y) is more selective to xylenes than medium pore zeolite.

The selectivity towards the dealkylation is found to be under control up to the above threshold for Ni addition, which was also reported by Babu et al. [21]. They studied the C_8 aromatics conversion over 0.1 wt.% Pt/HZSM-5, 0.2 wt.% NiH-ZSM-5 and 0.05 wt.% Pt–0.2 wt.% Ni/ZSM-5 and found that incorporation of Ni and Pt enhances the efficiency of the catalysts in producing *p*-xylene. Simultaneously, these metals suppress the disproportionation and loss of xylenes to toluene and trimethylbenzene.

3.2.4. *Effect of temperature on product selectivity*

The effect of temperature on the selectivity of individual xylene isomers over typical catalysts B_3 and M_2 are shown in Table 4. The selectivity of the xylene isomers as well as conversion was found to decrease with increasing temperature over the catalytic systems. The fall in selectivity of isomerized products (xylenes) is more than that of disproportionation and transalkylation products. The selectivity of TMB, ET, DEB and C_8 naphthenes are found to be increasing with temperature and Ni content. The lower temperature favors the isomerization and hydrogenation of C_8 aromatic (the corresponding products are primary). Transalkylation (ET) and cracking of C_8 naphthenes are secondary products. The secondary nature of these products was quite expected since ethylbenzene–xylenes transalkylation is necessarily consecutive to isomerization and cracking is consecutive to naphthenes formation. It can be concluded that reactions 2 and 3 occur through acid catalysis and hydrogenation through metal catalysis. The second part of reaction 4 (isomerization of N_8), reaction 1 (isomerization) and reaction 5 (cracking) occurs through bifunctional catalysis [22]. At first, the aromatic ring is partially hydrogenated via a ring contraction and expansion mechanism to obtain xylene isomers (Scheme 1). A complete hydrogenation of the aromatic ring would not necessarily be a disadvantage as the cycloalkanes can be recycled. On the other hand, the irreversible ring opening leads to loss of aromatic. Therefore, an appropriate ratio between acidic and metallic functions of the catalyst is required in order to obtain a good selectivity.

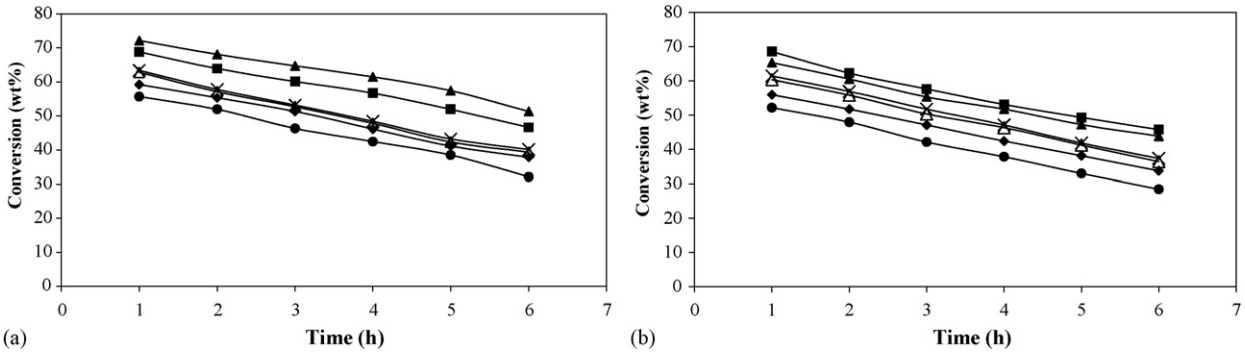

Fig. 8. (a) Effect of time-on-stream over B series catalysts: (♦) B_1, (■) B_2, (▲) B_3, (×) B_4, (△) B_5 and (●) B_6. (b) Effect of time-on-stream over M series catalysts: (♦) M_1, (■) M_2, (▲) M_3, (×) M_4, (△) M_5 and (●) M_6.

Table 4
Effect of temperature on the product selectivity of ethylbenzene over B_3 and M_2 catalysts

Catalyst	Temperature (°C)	Benzene	Toluene	Xylene	ET	TMB	DEM	Naphthenes
B_3	250	15.8	4.3	55.8	3.7	2	10.3	8
	300	13.8	3.6	53.9	4.7	2.2	13	10.1
	350	11	3.5	51.5	5.8	2.3	14.4	11.7
	400	10	2.9	47.6	7.3	3.1	15	14.2
M_2	250	14.4	3.5	54.9	3.2	3	9.7	11
	300	11.5	2.6	53.7	4.2	3.3	11.2	15.1
	350	10.6	2.2	48.6	6	3.4	13	16.1
	400	9.8	2.0	41.1	6.5	4.9	17.2	18.4

ET: ethyltoluene; TMB: trimethylbenzene; DEB: diethylbenzene.

3.2.5. *Effect of time-on-stream*

The sustainability of B and M series catalysts in EB hydroisomerization reaction is studied by conducting the time-on-stream for 6 h at 300 °C and the EB conversions are presented in Fig. 8(a) and (b), respectively. All the catalysts show a decline in conversion when increasing the time-on-stream. Catalysts B_3 of B series and M_2 of M series show the minimum fall in their activity. Catalysts without Ni (B_1 and M_1) and Ni only loaded catalysts (B_6 and M_6) show the maximum fall in activity during the time-on-stream. The higher sustainability of the catalysts B_3 and M_2 is explained in terms of catalytically active bimetallic particles formed and a more optimized metal–acid site ratio. The deactivation of the catalysts can be accounted in terms of coke formation due to cracking, which blocks the active sites of the catalysts.

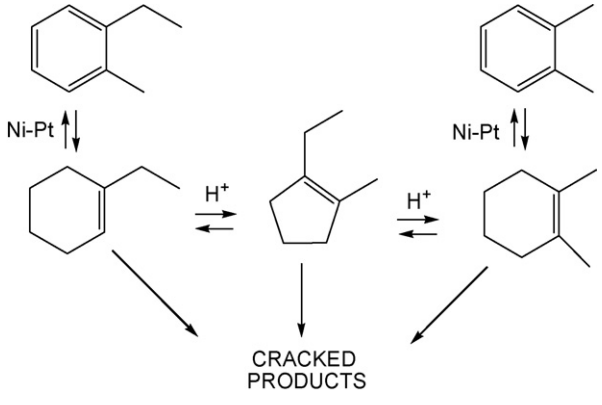

Scheme 1. Simplified scheme of bifunctional hydroisomerization of ethylbenzene.

4. Conclusion

The XRD and TEM analysis shows the formation of bimetallic (Ni–Pt) particles of nanoscale size. The ESCA study reveals that complete reduction of Ni up to 0.3 and 0.1 wt.% over 0.1 wt.% Pt loaded β and mordenite, respectively. The acidity measurements by both TPD-NH_3 and pyridine adsorbed FT-IR spectral studies show that some of the acid sites are occupied by the added Ni species. Because of the best metal–acid balance between bimetallic particles and acid sites of the support, catalysts 0.3 wt.% Ni–0.1 wt.% Pt/H-β and 0.1 wt.% Ni–0.1 wt.% Pt/Mordenite display an enhanced activity, isomerization selectivity and sustainability of the catalyst for EB hydroisomerization. Further Ni addition leads to a fall in activity of the catalysts. Also, the β-zeolite-based catalysts are found to be more suitable catalysts for EB hydroisomerization than mordenite-based catalysts.

References

[1] P.B. Weisz, Advances in Catalysis, vol. 13, Academic Press, London, 1962, p. 137.
[2] R.J. Toylor, R.H. Petty, Appl. Catal. 119 (1994) 121.
[3] A. Gil, A. Diaz, L.M. Gandia, M. Montes, Appl. Catal. 109 (1994) 167.
[4] D.L. Hong, H. Berndt, H. Missner, E. Schereier, J. Volter, van Santen, Ind. Eng. Chem. Res. 34 (1995) 55.
[5] J.M. Ward, Fuel Process. Techrol. 32 (1993) 55.
[6] F. Moreau, N.S. Gnep, S. Lacombe, E. Merlen, M. Guisent, Appl. Catal. 230 (2002) 253.

[7] K.H. Robschlger, E.G. Christoffel, Ind. Eng. Chem. Prod. Res. Dev. 18 (1979) 947.
[8] M.A. Jordao, V. Simoes, A. Montres, D. Cardoso, Stud. Surf. Sci. Catal. 130 (2000) 2387.
[9] A. Geetha Bhavani, D. Karthekayen, A. Sreenivasa Rao, N. Lingappan, Catal. Lett. 103 (2005) 89.
[10] P. Canizares, A. de Lucas, F. Dorado, A. Duran, I. Asencio, Appl. Catal. 169 (1998) 137.
[11] D.J. Ostard, L. Kustov, K.R. Poeppelmeier, W.M.H. Sachtler, J. Catal. 133 (1992) 342.
[12] M.A. Arribas, F. Marquez, A. Martinez, J. Catal. 190 (2000) 309.
[13] Ch. Minchev, V. Knazirev, L. Kosova, V. Pechev, W. Grunsser, F. Schimidt, in: L.V.C. Rees (Ed.), Proceedings of the Fifth International Conference on Zeolite, Heydon, London, 1980, p. 335.
[14] S. Narayanan, Zeolites 4 (1984) 231.
[15] S. Xiao, Z. Meng, J. Chem. Soc., Faraday Trans. 90 (1994) 2591.
[16] L.-J. Leu, L.-Y. Hov, B.-C. Kang, C. Li, S.-T. Wu, T.-C. Wu, Appl. Catal. 69 (1991) 49.
[17] S.M. Csisery, J. Catal. 19 (1970) 394.
[18] S.M. Csisery, J. Catal. 23 (1971) 124.
[19] C.V.V. Satyanarayana, D.K. Chakrabarty, Appl. Catal. 66 (1990) 1.
[20] L.D. Fernandes, J.L.F. Monteiro, E.F. Sousa-Aguiar, A. Martinez, A. Corma, J. Catal. 177 (1998) 363.
[21] G.P. Babu, M. Santra, V.P. Shiralkar, P. Ratnasamy, J. Catal. 100 (1986) 458.
[22] J.M. Silva, M.F. Ribeiro, F.R. Ribeiro, E. Benazzi, M. Guisent, Appl. Catal. 125 (1995) 15.